

Letter

Urban Growth Dynamics in Perth, Western Australia: Using Applied Remote Sensing for Sustainable Future Planning

Andrew MacLachlan ^{1,*}, Eloise Biggs ², Gareth Roberts ¹ and Bryan Boruff ²

¹ Geography and Environment Department, The University of Southampton, University Road, Southampton SO17 1BJ, UK; G.J.Roberts@soton.ac.uk

² School of Agriculture and Environment, The University of Western Australia, Crawley WA 6009, Australia; eloise.biggs@uwa.edu.au (E.B.); bryan.boruff@uwa.edu.au (B.B.)

* Correspondence: A.C.MacLachlan@soton.ac.uk; Tel.: +44-023-8059-9586

Academic Editors: Andrew Millington, Harini Nagendra and Monika Kopecka

Received: 16 December 2016; Accepted: 18 January 2017; Published: 24 January 2017

Abstract: Earth observation data can provide valuable assessments for monitoring the spatial extent of (un)sustainable urban growth of the world's cities to better inform planning policy in reducing associated economic, social and environmental costs. Western Australia has witnessed rapid economic expansion since the turn of the century founded upon extensive natural resource extraction. Thus, Perth, the state capital of Western Australia, has encountered significant population and urban growth in response to the booming state economy. However, the recent economic slowdown resulted in the largest decrease in natural resource values that Western Australia has ever experienced. Here, we present multi-temporal urban expansion statistics from 1990 to 2015 for Perth, derived from Landsat imagery. Current urban estimates used for future development plans and progress monitoring of infill and density targets are based upon aggregated census data and metrics unrepresentative of actual land cover change, underestimating overall urban area. Earth observation provides a temporally consistent methodology, identifying areal urban area at higher spatial and temporal resolution than current estimates. Our results indicate that the spatial extent of the Perth Metropolitan Region has increased 45% between 1990 and 2015, over 320 km². We highlight the applicability of earth observation data in accurately quantifying urban area for sustainable targeted planning practices.

Keywords: unsustainable development; urban expansion; remote sensing; Landsat

1. Introduction

Over the last 15 years, Perth has experienced exponential economic growth with Gross State Product (GSP) increasing 218% [1]. Originally labelled as the 'Cinderella State' due to its remote location and perceived neglect from the rest of Australia, Western Australia (WA) has experienced sustained discovery and extraction of natural resources since the beginning of the 21st century [2]. In response to a growing resource sector, the city of Perth has undergone extensive urban expansion at what Dhakal (2014) identified as an unsustainable rate [3]. To this end, the Western Australian Planning Commission (WAPC) identified that Perth's urban footprint has increased from 631 km² to 870 km² in the 10 years between 2002 and 2012 [4,5]. However, these figures should be considered with caution as data used in early estimates represent land parcel (Cadastral) valuations only (provided by the Western Australian Value General's Office), with later estimates (from 2009) based on multiple urban zoning classifications, and more recently (from 2010) spatial modelling taking into account land valuation and zoning [6,7]. The use of varied data and methods impacts confidence in the ability of the Commission's

estimates to represent actual change in urban extent, especially when urban zoning information includes land identified for growth but not necessarily developed. Such inconsistencies could have potential to misinform future development decisions. Consequently, here we present a spatiotemporal assessment of change in areal urban growth based upon medium resolution remote sensing through a single classification model. This provides the first accurate depiction of urban expansion for one of the world's fastest growing cities—Perth, WA. We present our findings and discuss the implications of more accurately classified urban extents in facilitating scientifically evidence-based adaptive and targeted planning policies to help reduce environmental and socio-economic consequences of poorly planned development.

1.1. Earth Observation for Monitoring Urban Change

Mapping the spatial extent and temporal profile of urban growth from medium resolution satellite imagery facilitates a consistent, detailed characterisation of the actual urban footprint of a city [8,9]. Other conventional spatial datasets such as Cadastral data provide information on freehold and Crown land parcel boundaries including attributes such as ownership and value for a singular temporal period [10]. However, attributed data for a singular year provides an ineffective portrayal of actual parcel land cover and temporal change. Thus, the methods and results presented in this study provide foundational information for the development of planning regulations that ensure sustainable growth of our cities, particularly in the reduction of environmental risks from ever-increasing expansion along the wildland–urban interface [11]. Specifically, Earth Observation (EO) data allows spatially detailed identification of locations where (un)sustainable urban growth is occurring which enables expansion limits to be imposed through targeted policies [12]. In this theme, Schneider et al. (2005) determined the spatial distribution of development zones from 1978 to 2002 in Chengdu, Sichuan province, China in response to the Go West policy of the 1990s, aimed at economically boosting the West of the country [13]. Whilst the policy was successful in raising Gross Domestic Product (GDP) levels, urbanisation concurrently increased, generating issues of urban management, including service, infrastructure and resource deficiency. Their results indicated spatial clustering, specialisation of land use and peri urban development (not considered by the original policy) which were subsequently used to tailor policy in remediating issues, facilitating sustainable future urban development [13,14]. Similarly, Hepinstall-Cymerman et al (2013) used classified Landsat data to monitor urban growth in regards to imposed growth boundaries in the Central Puget Sound, Washington, USA [15]. Surprisingly, more new development occurred outside the growth boundaries than inside within their last time period, illustrating the ineffectiveness of the imposed policy leading to economic and ecological consequences, including a loss of avian diversity in native forest species [15,16]. These studies highlight the potential effectiveness of EO data in consistently monitoring the spatiotemporal dynamics of urban development for applied policy outcomes and ensuring sustainable future planning decisions, for which such outputs are unachievable from traditional datasets.

1.2. The Case of Perth

Perth's dramatic urban expansion can be attributed to Australia's minerals and energy boom commencing at the turn of the century. Queensland (QLD) and WA were at the forefront of the boom contributing the largest proportion of the nation's resources output, valued at 3.3% of GDP [1]. In WA, mining and petroleum extraction dominate exports, peaking at 95% of the state's export earnings between 2010 and 2011 [17]. The increase in extraction was predominantly attributable to greater demand for raw materials from China, resulting in steady growth of the WA mineral and petroleum industry from AUD 4.7 billion in 1996 to a peak of AUD 121.6 billion mid-2013. However, in 2009, a 10.3% reduction in the overall value of mineral and petroleum resources resulted from falling commodity prices and the 2007–2009 global financial crisis [17]. Again in 2012, a further 9% reduction in resource value was observed as uncertainty in global economic conditions increased [17]. The largest decline to date occurred between 2014 and 2015, with an additional 22% reduction in the value of

mineral and petroleum resources as a result of surplus capacity, decreased demand, and decline in the value of the Australian dollar [17]. The temporal trend in resource value indicates a stagnation and decline since late 2013 (Figure 1).

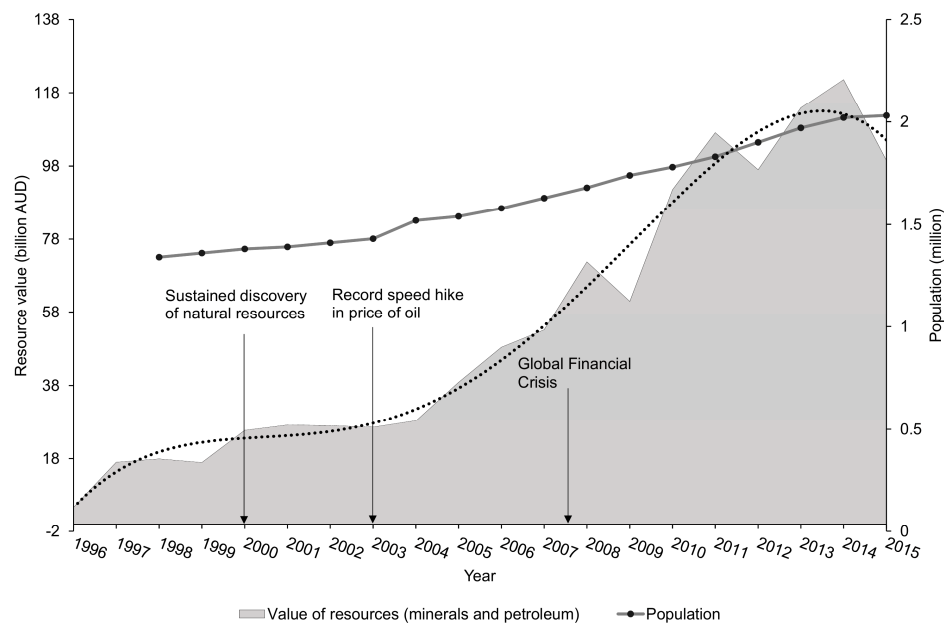


Figure 1. Timeline of natural resource value (based on Department of Mines and Petroleum annual reports) fitted with a fourth order polynomial trend line and population (based on Australian Bureau of Statistics data) also indicating key milestones.

Perth is described as one of the most isolated cities in the world (pop. > 1 million) and was Australia's fastest growing metropolis between 2007 and 2014; however, subsequent to a decline in natural resource value, a slowdown in population expansion soon followed (Figure 1) [2]. As a result, 2015 population statistics highlight the lowest population increase since records began with a 0.5% increase from the previous year [1,2]. In comparison to other Australian state capitals, based on the Australian Bureau of Statistics (ABS) 2011 population grid, Perth exhibits a relatively sparse spatial distribution of population with a maximum population density of only 3662 people per square kilometre (Melbourne 10,827; Sydney 14,747). Such low density population has generated high demand for dispersed housing, amenities and services, and has influenced changes to Perth's land use patterns in a non-strategic, "lot-by-lot fashion" based on a car-dependent lifestyle [3]. Anthropogenic modifications of the landscape from vegetation cover to human-made impervious surfaces represent a critical driving force in both local and global environmental change [18,19]. For example, abrupt, poorly planned and uncontrolled urban expansion can lead to environmental impacts which degrade ecological systems including habitat fragmentation and socio-economic issues that deteriorate efficiency of amenity provisioning, both of which can exacerbate localised climate change [11,20]. Identifying impacts of Land Use and Land Cover (LULC) change on socio-ecological systems is vital for future sustainable urban development; as reflected in the "sustainable cities and communities" 2030 sustainable development goal and the effective land use planning criteria of the City Resilience Framework (CRF) [19,21]. It is essential for Perth to adapt current practices of outward suburban expansion to achieve more sustainable urban growth and become city-smart for accommodating the predicted additional half a million new residents by 2031, which will result in an overall population exceeding 2.2 million [5].

2. Materials and Methods

2.1. Data Preprocessing

EO data have been extensively used to monitor the sustainability of urban areas [22,23]. However, accurate identification and temporal monitoring of urban land is frequently precluded due to the coarse resolution (300 m–1 km) of a number of commonly used remotely sensed datasets including night time lights (1 km) and the Moderate Resolution Imaging Spectroradiometer (MODIS) land cover product (0.083°) [22,24]. Whilst 30 m resolution data (e.g., Landsat) are more suitable to detect nuances of urban development the majority of studies and classified products which have used these finer resolution products implement large temporal windows, negating the possibility of detailed temporal urban characterisation e.g., GloeLand30 [25–29]. This research provides the first comprehensive temporal evolution analysis quantifying land cover change and associated urban expansion for the Perth Metropolitan Region (PMR) using 30 m Landsat imagery, the longest temporal record of medium spatial resolution imagery, for seven sequential time snapshots between 1990 and 2015.

Cloud free imagery was acquired in or close to the month of July for 1990, 2000, 2003, 2005, 2007, 2013 and 2015. Analysis of imagery acquired from WA winter season coincided with peak green-up which provided the greatest contrast between spectrally similar surfaces (e.g., bare earth and urban) [30–32]. Imagery date selection was founded upon the strong positive relationship between Australian soil moisture (related to rainfall) and the Normalised Difference Vegetation Index (NDVI) [33], which exhibits an approximate one month lag between peak soil moisture and peak NDVI [33].

Productive photosynthesising plants use energy in the visible red (VIS) portion of the electromagnetic spectrum whilst reflecting in the near-infrared (NIR) region. NDVI ((NIR -VIS)/(NIR + VIS)) is a representative measure of growth allowing for the identification of green, healthy vegetation [33–35], as illustrative of Southwest WA's winter months. A total of 14 images from Landsat 5 Thematic Mapper (TM) (eight images), Landsat 7 Enhanced Thematic Mapper Plus (ETM+) (two images) and Landsat 8 Operational Land Imager (OLI) (four images) were acquired for the specified years. Seamless images were produced based on Voroni diagrams that locate the bisector between images; adjacent edges were identified as seamlines constraining effective mosaic polygons that specify inclusion pixels for the final mosaicked product, permitting less visible boundaries through blending overlapping pixels [36]. Mosaicked images were subsequently clipped to the original PMR study area boundary.

The atmospherically corrected Landsat data used in this study were obtained from the Landsat Ecosystem Disturbance Adaptive Processing System (LEDAPS) and the Landsat 8 Surface Reflectance (L8SR) algorithm [37,38]. Some inherent residual noise remained, for example, due to the differences in modelled atmospheric correction parameters [39]. To correct for this, surface reflectance values were standardised as¹:

$$p_{i,b} = \frac{p_{x,b}}{\max_b} \quad (1)$$

where $p_{i,b}$ is the standardised pixel value i , from band b based on the original surface reflectance x , standardised through division of a priori specific upper reflectance limit for each band (\max_b): 0.1 (blue; 0.48 μm), 0.11 (green; 0.56 μm), 0.12 (red; 0.66 μm), 0.225 (near-infrared; 0.84 μm), 0.205 (shortwave-infrared; 1.65 μm), 0.150 (shortwave-infrared 2; 2.22 μm) [40]. Standardised values were then normalised per pixel j through cross band sum division:

$$p_{j,b} = \frac{p_{i,b}}{\sum_i p_{i,b}} \quad (2)$$

¹ Using the Interactive Data Language (IDL) version 8.3

where $\sum_i p_{i,b}$ is the sum of each standardised pixel across all bands [40]. Normalised Landsat data obtained a statistically significant reduction of spectral variation per land cover class within (inter) and between (intra) each image (see Figure S1).

2.2. Data Classification

The normalised Landsat imagery was classified using the Import Vector Machine (IVM) which builds upon the popular Support Vector Machine (SVM) methodology² [41]. In order to obtain the optimum classification, the IVM algorithm explores all possible subsets of training data for optimal selection (termed import vectors) which are derived through successively adding training data samples until a given convergence criterion is met [41]. Data samples are selected according to their contribution to the classification solution. However, a pure forward system is unable to remove import vectors that become obsolete after addition of other vectors. Therefore the implemented version of IVM utilised here is a hybrid forward/backward strategy that adds import vectors whilst concurrently testing if they can be removed in each step, thus leading to a sparse and more accurate solution [41]. Furthermore, the IVM selects data points from the entire distribution resulting in a smoother decision boundary which is based on the optimal separating hyperplane in multidimensional space compared to that of SVM algorithms [42]. The benefits of the IVM algorithm have resulted in this approach being successfully applied in a number of studies (e.g., [42–45]) due to its accuracy and performance advantages over alternative methodologies including SVM and the traditional Maximum Likelihood (ML) classifiers [44,45].

Model training samples were selected using the July 2005 Landsat 5 TM image coinciding with the month post maximum rainfall of all considered Landsat 5 TM and 7 ETM+ to facilitate optimum spectral separability³ [33]. Land cover was defined as high albedo urban (e.g., concrete), low albedo urban (e.g., asphalt) or other. Two urban classes were initially identified in order to reduce confusion between spectrally similar classes (e.g., urban and bare earth) being merged post-classification to represent complete urban coverage [46]. For each class, 250 pixels were randomly selected as training data, which is consistent with Foody and Mathur (2006) and Pal and Mather (2003) (see Supplementary S2). Training data parametrised the IVM algorithm, creating a classification model of spectral profiles that are compared to Landsat spectral profiles for classification. The classification model was then applied to all Landsat 5 TM and Landsat 7 ETM+ images obtaining similar spectral wavebands, considered to be equivalent [47]. However, due to Landsat 8 OLI sampling different spectral regions, a new classification model was developed using the same training areas, as these were deemed to remain representative of the land cover, but with Landsat 8 OLI spectral wavebands [47,48]. Validation was performed through an accuracy assessment based on an independent dataset (Google Earth high resolution imagery) consistent with Landsat acquisition months following previously published methods (e.g., [22,49–53]). For each land use category, 50 pixels per class per year were visually identified and classified based on the majority land cover within the coincident Landsat pixel from Google Earth imagery for the available years: 2000, 2003, 2005, 2007, 2013 and 2015 consistent with recommended land cover accuracy sample size of Congalton (2001) [54].

3. Results

The spatial footprint of PMR development has increased 45% between 1990 and 2015, over 320 km² (Figures 2 and 3), with a 37% increase occurring since 2000. The classification accuracy assessment indicates an average overall accuracy of 84.1% and Kappa Coefficient of 0.73 being comparable to other studies (e.g., [52,55–57]) (see Tables S1 and S2). Urban expansion mirrors population increase

² Using the open source Environmental Mapping and Analysis Program version 2.1.1 (EnMAP)

³ Achieved in the ENvironment for Visualizing Images software version 5.2 (ENVI)

and as population growth has slowed, urban development has concurrently exhibited a levelling trend compared to expansion previously observed (Figure 3).

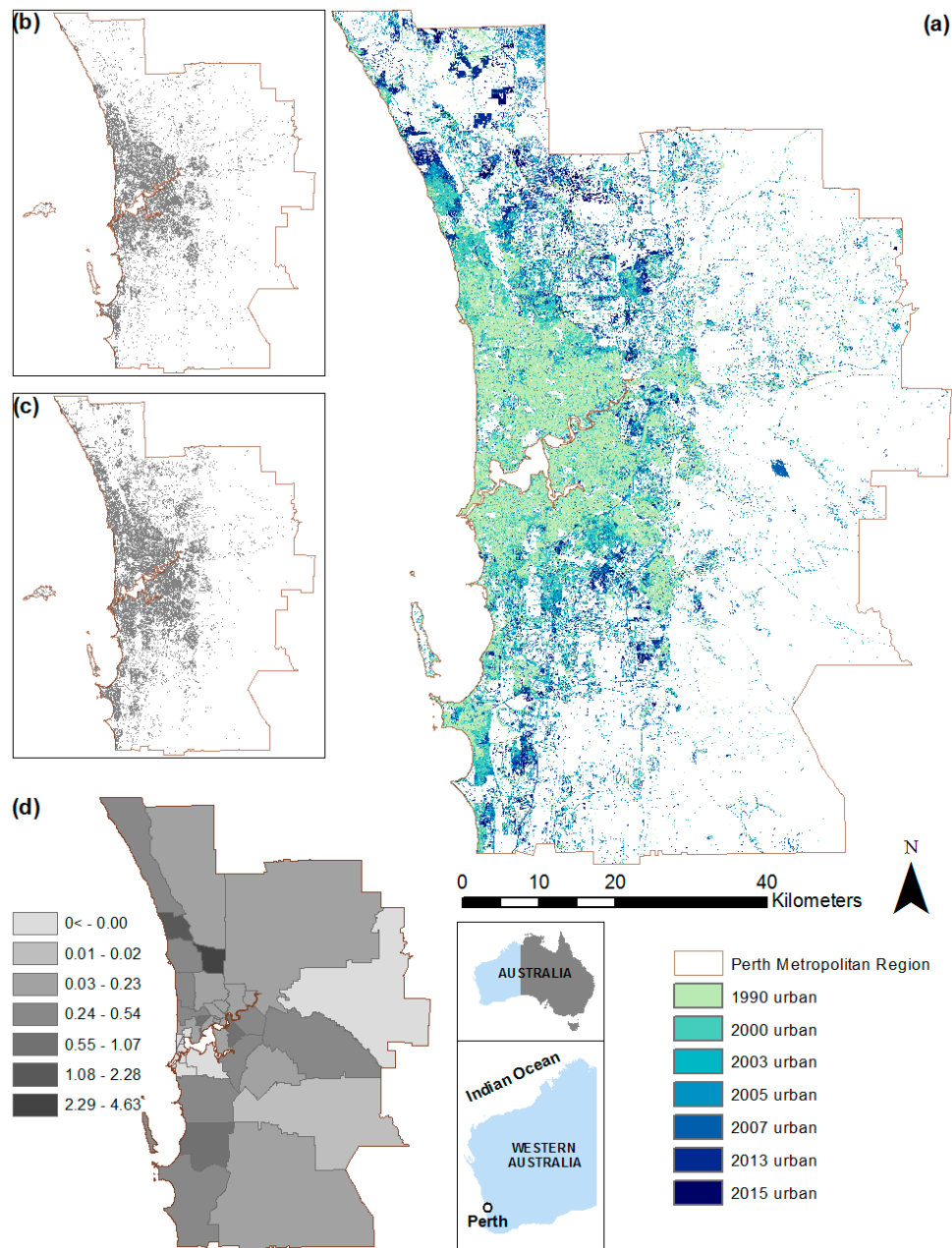


Figure 2. Urban expansion within the Perth Metropolitan Region (PMR) between 1990 and 2015. Vast urban growth has been observed in PMR with graduating colours exhibiting outward expansion (a); (b) and (c) exhibit static snapshots of urban extent from 2000 (b) and 2015 (c); whilst (d) depicts percentage of urban change per subnational administrative boundary (Local Government Area; LGA).

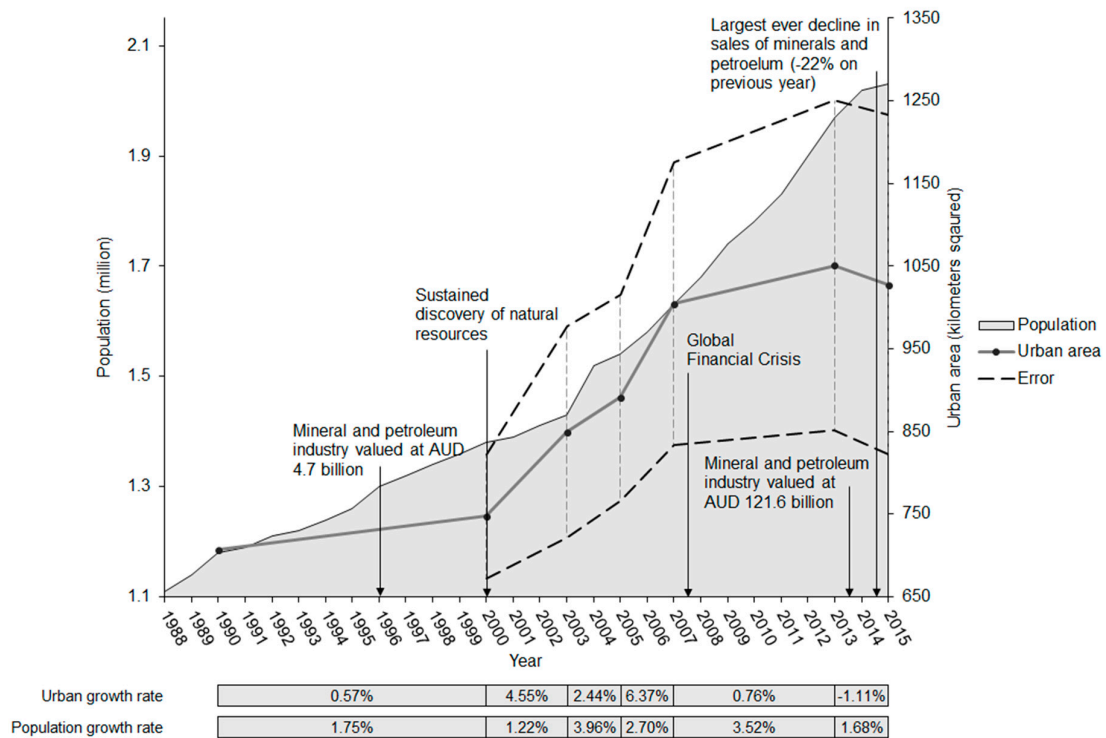


Figure 3. Time line of urban expansion in kilometers squared derived from Earth observation data with associated classification error derived from validation data (points indicating classified image years). Alongside population data in millions per year since 1988 (based on Australian Bureau of Statistics data, 2015 data is projected) with key natural resource milestones indicated, and average annual urban and average annual population growth rate indicated between classified image years.

WAPC’s urban estimates of the PMR from Directions 2031 (the strategic plan for the Perth and Peel region) were provided for comparison to those produced within this study⁴ [5]. WAPC’s estimates note an expansion from 637 km² to 813 km² between 2001 and 2012. Our results indicate an expansion of 747 km² to 1050 km² from 2000 to 2013 illustrating an overall underestimation by WAPC figures (Figure 4). Within suburban areas surrounding the two major cities in the metropolitan region, Perth and Fremantle, WAPC’s estimates underrepresent the amount of urban area derived from EO, being more pronounced in 2013 than 2000. The Local Government Area (LGA)⁵ of Stirling South Eastern represented the maximum overestimation in 2013 urban area with 34% (2000: 10%) additional urban area per km² of LGA established on a difference of 2.89 km², 40.2% (2000: 0.83 km², 15%) between EO data and WAPC’s estimates. Outer Northern and Southern LGA WAPC urban values were consistently underestimated, with the LGA of Belmont representing the maximum underestimation of percent per km² of LGA in 2013 with 24% (2000: 13%) due to a difference of 9.37 km², 40.39% (2000: 5 km², 26.46%). Prior to 2009, WAPC’s estimates were solely based upon land parcel valuations from the Western Australian Value General’s Office, consequently valuation thresholds designating land to urban may have been inappropriately applied to outer suburban LGAs, where land might be developed but less valuable than central LGAs.

For urban estimates post 2005, two urban land zones, urban and urban deferred, are used within the Perth Metropolitan Region Scheme (MRS), the division of the State Planning Policy Framework applicable to the PMR, pursuant to the Planning and Development Act (2005) that inform recent WAPC

⁴ Analysed in ArcGIS version 10.2.2

⁵ Outlines of LGAs are displayed in Figure S2

land parcel based estimates [58,59]. Urban land refers to locations where activities in line with urban development are permitted, but not necessarily constructed (e.g., housing and commercial use) whilst urban deferred represents land suitable for future development with remaining planning, servicing or environmental issues [59,60]. For land to be assigned urban deferred, it must obtain characteristics of the urban zone including being able to provide essential services, a logical progression of development, and able to satisfy regional requirements (e.g., roads and open spaces). The 2012 WAPC estimates were derived from stock of land zoned urban or urban deferred, cadastral land plot and value information, conditional subdivision approvals, and ongoing regional rezoning and subdivisions [61]. Similarly to 2000, valuation data may misrepresent suburban urban land cover resulting in overestimation. Inclusion of additional variables that are unrepresentative of actual land cover change (e.g., rezoning and conditional approvals) could exacerbate differences between WAPC and EO derived urban estimates (Figure 4b), leading to the potential confounding of errors in WAPC estimates.

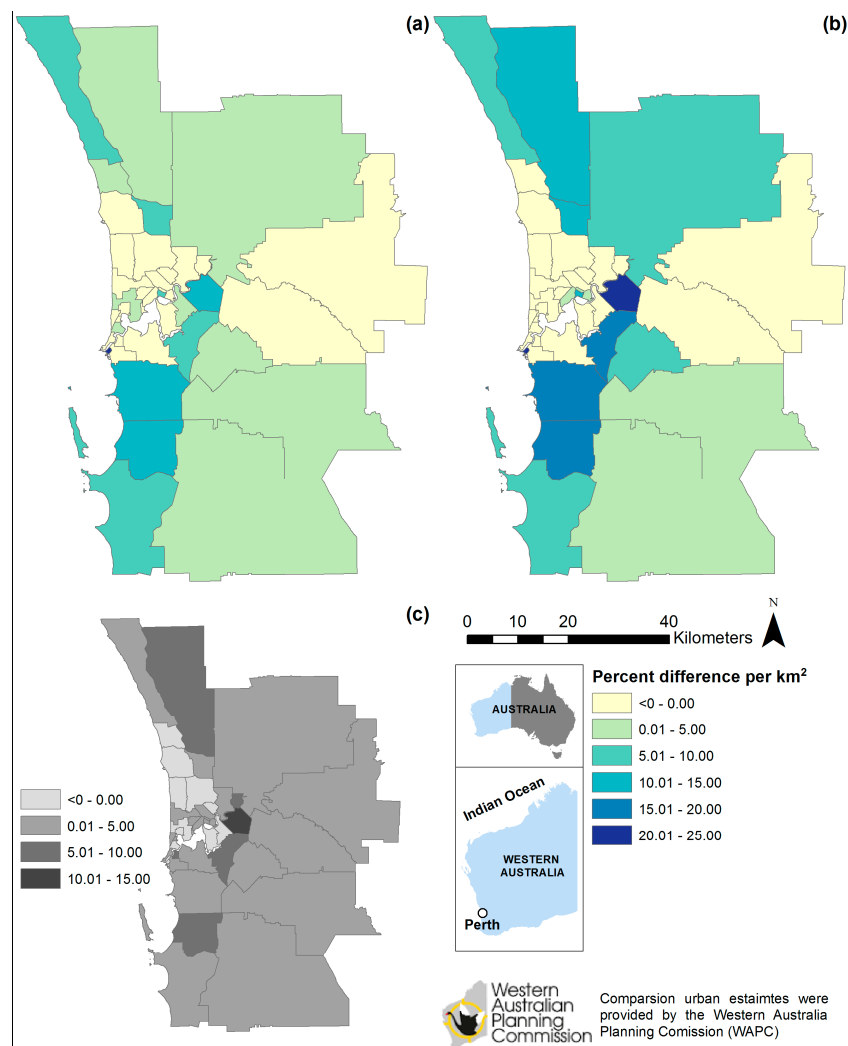


Figure 4. Percentage differences relative to local government area size, permitting a change metric standardised by Local Government Area (LGA) area between Earth Observation (EO) and the Western Australian Planning Commission’s (WAPC) urban estimates for: (a) 2000 (EO) and 2001 (WAPC) and (b) 2012 (WAPC) and 2013 (EO), whilst (c) depicts the percentage difference in the relative urban rate of change (km² per LGA area) between 2000 and 2013 (EO) and 2001 and 2012 (WAPC). Positive values indicate underestimation by WAPC whilst negative values represent overestimation by WAPC.

4. Discussion

WA state government planning documentation states that the majority of new development within the PMR has occurred as low-density suburban growth, responding to consumer preferences and market forces [4]. Additionally, sustainable policy objectives suggest that new development should be managed and focused on current communities, making the most efficient use of existing urban areas [4,5]. Planning policy research has highlighted issues of outward urban expansion as being costly in economic, environmental and social terms based on dispersed service requirements, habitat fragmentation and neighbourhood segregation [20]. Thus, urban expansion in the PMR may result in further economic, social and environmental costs associated with servicing and maintaining low-density lifestyles, owing to the rapid outward urban growth estimates between 2000 and 2007 [11,20].

In contrast, the witnessed slowdown of urban growth, population and natural resource value since 2013 indicates the possibility that the 'boom' of previous years has reached a turning point. Stagnation of urban growth implies that issues associated with spatially distributed urban areas might be contained to the current urban extent. Nevertheless, it is conceivable that prosperous future economic circumstances could initiate growth at a rate previously observed, and that the economic slowdown might be a temporary hiatus responding to current economic conditions [62]. For example, in 2014–2015, WA continued to attract the largest proportion of state mineral exploration expenditure at 58%, with QLD (the second ranked state) obtaining only 20% [17]. Furthermore, as of September 2015, WA had an estimated AUD 171 billion in mineral and petroleum projects under construction, with a further AUD 110 billion allocated for future expansion [17]. Comparatively, during the peak (mid-2013) in terms of total sales, WA only had an estimated AUD 160 billion worth of projects under construction and a further AUD 108 billion for future development [17]. Whilst 2014–2015 observed the greatest decline in total sales of resources, sustained investment and improved global economics could reinvigorate the industry and reinitiate urban expansion within the PMR.

Future development (urban and urban deferred) is guided by Directions 2031 amending the MRS and local planning schemes [5,63–66]. WAPC aims to achieve 47% of future development as infill and a 50% increase in average residential density by 2050 of 10 dwellings per urban zoned hectare and 15 per new urban zoned hectare [5]. In monitoring progress towards the infill target, zoned development land within the PMR is considered, including residential, industrial and commercial land uses [4]. Densities are defined as infill or Greenfield if above or below an undocumented residential threshold from census data [60]. Initial results from delivering directions 2031, 2014 report indicate the requirement of a significant increase in infill development if the above targets are to be met [67]. Similarly, average residential density monitoring has been achieved with land valuation data (from the Valuer General's Office) for major activity centres, being unrepresentative of actual density change and providing an incomplete metropolitan comparison [67]. Inclusion of EO data would permit quantitative evidence of urban expansion, infill and density at a higher spatial and temporal frequency than current census based estimates. This would facilitate credible, evidence-based efficient targeted action founded upon improved representative urban area, insuring infill and density attainment. In this theme, Schneider et al. (2005) and Hepinstall-Cymerman et al. (2013) used spatial metrics (e.g., urban area mean patch size) based on classified Landsat data in either pre-defined census units [15] or development corridors [13] to monitor development type (infill or expansion) over time for adapting inappropriate static urban development policy. Using EO derived land cover data in this manner aids in understanding dynamics of the urban environment through monitoring, planning and mitigating land use changes that impact natural assets and increase vulnerability of city systems [14,15,68]. Information of this sort aligns with criteria of the CRF in improving city resilience from effective land use planning, possible at lower expense and higher temporal frequencies than in situ measurements [21].

The universal methodology implemented within this research lends itself to credibly inform policy in a similar manner in other global cities through monitoring urban expansion in order to identify rapid,

unsustainable development. For example, Jakarta, obtaining the world's second largest urban area with a population of 28 million, has yet to have any quantitative urban area delineation [69,70]. Identification of actual urban growth in developing cities is vital to city planners, environment managers and policy makers due to the difference between planned growth and actual growth [14]. Such information could be of critical importance for regulating urban expansion due to extreme poverty and high level of risk to environmental hazards, such as that posed from flooding [71,72]. EO data presents many opportunities for added value within urban planning policy, and additional analyses could be pursued into specific human-induced environmental issues, such as detecting thermal changes in the urban environment for planning issues associated with urban heat islands (e.g., cooling provisions) and their impact on human health (e.g., air quality).

5. Recommendations

Consistent and accurate LULC estimates are a vital aspect of sustainable urban development throughout the world, especially considering the predicted additional 2.5 billion city dwellers by 2050. LULC models that require agents that are representative of land use decisions can often fail in practicality due to the difficulty in quantifying driving forces of change and multi-level relationships. Models of this nature are also temporally independent, with each annual iteration implementing new data or data not representative of actual LULC change. EO data provides a replicable detailed representation of the complete urban extent requiring no additional data. The use and application of EO data reported within this paper highlights several improvements to WAPC policy for consistent urban area estimations with associated accuracy measures. Therefore it is recommended that planning authorities, such as WAPC, integrate EO data to achieve the following: (1) provide scientific urban estimates based on a temporally consistent model within future regional structure plans, metropolitan region and local planning schemes; (2) monitor infill development at a higher temporal frequency than census years for policy targeting to meet key goals; (3) monitor urban density through areal urban expansion compared to current metrics using land valuations; and (4) restrict development based on temporal urban analysis that degrades amenity efficiency and ecological systems whilst promoting development in locations to maximise efficiency and long-term sustainability. Additional EO datasets (e.g., finer resolution Sentinel 2 satellite imagery or aerial imagery) could be used to refine planning decisions based on areas of concern identified from Landsat. For example, finer spatial resolution datasets could facilitate enhanced feature extraction, optimising sustainable planning decisions through the identification of candidate infill sites. EO data of this nature provides an essential tool for timely planning policy that is adaptive to changes in urban landscape to mitigate socio-environmental issues associated with poorly planned urban areas for the future sustainability of our cities.

Supplementary Materials: The following are available online at www.mdpi.com/2073-445X/6/1/9/s1. Additional methodological detail, full accuracy results and Local Government Area (LGA) outlines are reported in the supplementary documentation. Figure S1 Inter year classification reflectance variation categorised by classified output for each spectral band for: pre (a) and post (b) normalisation correction. Table S1 Classification accuracy and associated Kappa Coefficient per year of classified Landsat. Table S2 Producer's and User's accuracy per year of classified Landsat imagery. Figure S2 Local Government Areas (LGAs) located in Perth Metropolitan Region (a); with (b) exhibiting LGAs South and West of the Swan River and (c) LGAs North and East of the Swan River. The classified data reported in this paper (doi:10.1594/PANGAEA.871017) are archived at <https://doi.pangaea.de/10.1594/PANGAEA.871017>, the pangea open access data publisher for earth and environmental science.

Acknowledgments: This work was supported by the Economic and Social Research Council [grant number ES/J500161/1]. We would like to thank the World University Network (WUN) for facilitating institutional visits, the United States Geological Survey (USGS) for providing Landsat surface reflectance data and the Western Australia Department of Planning, in particular Matt Devlin and Lisl van Aarde for urban estimates and supplementary planning information.

Author Contributions: All authors assisted in conceiving and designing the experiments lead by Andrew MacLachlan; Andrew MacLachlan performed the experiments and analyzed the data; Eloise Biggs, Gareth Roberts and Bryan Boruff contributed reagents/materials/analysis tools; Andrew MacLachlan wrote the paper with input and revisions from Eloise Biggs, Gareth Roberts and Bryan Boruff.

Conflicts of Interest: The authors declare no conflict of interest and the founding sponsors had no role in the design of the study; in the collection, analyses, or interpretation of data; in the writing of the manuscript, and in the decision to publish the results.

References

1. ABS *Australian National Accounts 1988–2015*; Australian Bureau of Statistics: Belconnen, ACT, Australia, 2015.
2. Kennewell, C.; Shaw, B.J. Perth, Western Australia. *Cities* **2008**, *25*, 243–255. [[CrossRef](#)]
3. Dhakal, S.P. Glimpses of Sustainability in Perth, Western Australia: Capturing and Communicating the Adaptive Capacity of an Activist Group. *Cons. J. Sustain. Dev.* **2014**, *11*, 167–182.
4. *Western Australian Planning Commission Perth and Peel @ 3.5 Million*; Department of Planning, Government of Western Australia: Perth, WA, Australia, 2015.
5. *Western Australian Planning Commission Directions 2031 and beyond: Metropolitan Planning beyond the Horizon*; Department of Planning, Government of Western Australia: Perth, WA, Australia, 2010.
6. *Western Australian Planning Commission Urban Growth Monitor: Perth Metropolitan, Peel and Greater Bunbury Regions 2009*; Department of Planning, Government of Western Australia: Perth, WA, Australia, 2009.
7. *Western Australian Planning Commission Urban Growth Monitor: Perth Metropolitan, Peel and Greater Bunbury Regions 2010*; Department of Planning, Government of Western Australia: Perth, WA, Australia, 2010.
8. Angiuli, E.; Trianni, G. Urban Mapping in Landsat Images Based on Normalized Difference Spectral Vector. *IEEE Geosci. Remote Sens. Lett.* **2013**, *11*, 661–665. [[CrossRef](#)]
9. Bagan, H.; Yamagata, Y. Landsat analysis of urban growth: How Tokyo became the world’s largest megacity during the last 40years. *Remote Sens. Environ.* **2012**, *127*, 210–222. [[CrossRef](#)]
10. Thompson, R.J. A model for the creation and progressive improvement of a digitalcadastral data base. *Land Use Policy* **2015**, *49*, 565–576. [[CrossRef](#)]
11. Turner, B.; Lambin, E.; Reenberg, A. The emergence of land change science for global environmental change and sustainability. *Proc. Natl. Acad. Sci. USA* **2010**, *103*, 13070–13075. [[CrossRef](#)] [[PubMed](#)]
12. Bettencourt, L.; West, G. A unified theory of urban living. *Nature* **2010**, *467*, 9–10. [[CrossRef](#)] [[PubMed](#)]
13. Schneider, A.; Seto, K.C.; Webster, D.R. Urban growth in Chengdu, western China: Application of remote sensing to assess planning and policy outcomes. *Environ. Plan. B Plan. Des.* **2005**, *32*, 323–345. [[CrossRef](#)]
14. Patino, J.E.; Duque, J.C. A review of regional science applications of satellite remote sensing in urban settings. *Comput. Environ. Urban Syst.* **2013**, *37*, 1–17. [[CrossRef](#)]
15. Hepinstall-Cymerman, J.; Coe, S.; Hutyra, L.R. Urban growth patterns and growth management boundaries in the Central Puget Sound, Washington, 1986–2007. *Urban Ecosyst.* **2013**, *16*, 109–129. [[CrossRef](#)]
16. Hepinstall, J.A.; Alberti, M.; Marzluff, J.M. Predicting land cover change and avian community responses in rapidly urbanizing environments. *Landsc. Ecol.* **2008**, *23*, 1257–1276. [[CrossRef](#)]
17. *Western Australian Mineral and Petroleum Statistics Digest 1984–2015*; Department of Mines and Petroleum, Government of Western Australia: Perth, WA, Australia, 2015.
18. Kalnay, E.; Cai, M. Impact of urbanization and land-use change on climate. *Nature* **2003**, *423*, 528–531. [[CrossRef](#)] [[PubMed](#)]
19. Vitousek, P.; Mooney, H.; Lubchenco, J.; Melillo, J. Human Domination of Earth Ecosystems. *Science* **1997**, *277*, 494–498. [[CrossRef](#)]
20. Downs, A. Smart Growth: Why We Discuss It More than We Do It. *J. Am. Plan. Assoc.* **2005**, *71*, 367–378. [[CrossRef](#)]
21. *ARUP City Resilience Framework—100 Resilient Cities*; The Rockefeller Foundation: New York, NY, USA, 2015.
22. Song, X.-P.; Sexton, J.O.; Huang, C.; Channan, S.; Townshend, J.R. Characterizing the magnitude, timing and duration of urban growth from time series of Landsat-based estimates of impervious cover. *Remote Sens. Environ.* **2016**, *175*, 1–13. [[CrossRef](#)]
23. Li, X.; Gong, P.; Liang, L. A 30-year (1984–2013) record of annual urban dynamics of Beijing City derived from Landsat data. *Remote Sens. Environ.* **2015**, *166*, 78–90. [[CrossRef](#)]
24. Potere, D.; Schneider, A.; Angel, S.; Civco, D. Mapping urban areas on a global scale: Which of the eight maps now available is more accurate? *Int. J. Remote Sens.* **2009**, *30*, 6531–6558. [[CrossRef](#)]
25. Hu, Y.; Jia, G.; Hou, M.; Zhang, X.; Zheng, F.; Liu, Y. The cumulative effects of urban expansion on land surface temperatures in metropolitan Jingjintang, China Yonghong. *J. Geophys. Res. Atmos.* **2015**, *120*, 9932–9943. [[CrossRef](#)]

26. Masek, J.G.; Lindsay, F.E.; Goward, S.N. Dynamics of urban growth in the Washington DC metropolitan area, 1973–1996, from Landsat observations. *Int. J. Remote Sens.* **2000**, *21*, 3473–3486. [[CrossRef](#)]
27. Van de Voorde, T.; Jacquet, W.; Canters, F. Mapping form and function in urban areas: An approach based on urban metrics and continuous impervious surface data. *Landsc. Urban Plan.* **2011**, *102*, 143–155. [[CrossRef](#)]
28. Xian, G.; Homer, C.; Bunde, B.; Danielson, P.; Dewitz, J.; Fry, J.; Pu, R. Quantifying urban land cover change between 2001 and 2006 in the Gulf of Mexico region. *Geocarto Int.* **2012**, *27*, 479–497. [[CrossRef](#)]
29. Suarez-Rubio, M.; Lookingbill, T.R.; Elmore, A.J. Exurban development derived from Landsat from 1986 to 2009 surrounding the District of Columbia, USA. *Remote Sens. Environ.* **2012**, *124*, 360–370. [[CrossRef](#)]
30. Herold, M.; Gardner, M.; Hadley, B.; Roberts, D. The spectral dimension in urban land cover mapping from high-resolution optical remote sensing data. In Proceedings of the 3rd Symposium on remote Sensing of Urban Areas, Istanbul, Turkey, 11–13 June 2002; Volume 6, pp. 1–8.
31. Varshney, A.; Rajesh, E. A Comparative Study of Built-up Index Approaches for Automated Extraction of Built-up Regions From Remote Sensing Data. *J. Indian Soc. Remote Sens.* **2014**, *42*, 659–663. [[CrossRef](#)]
32. Lu, D.; Moran, E.; Hetrick, S. Detection of impervious surface change with multitemporal Landsat images in an urban-rural frontier. *ISPRS J. Photogramm. Remote Sens.* **2011**, *66*, 298–306. [[CrossRef](#)] [[PubMed](#)]
33. Chen, T.; de Jeu, R.A.M.; Liu, Y.Y.; van der Werf, G.R.; Dolman, A.J. Using satellite based soil moisture to quantify the water driven variability in NDVI: A case study over mainland Australia. *Remote Sens. Environ.* **2014**, *140*, 330–338. [[CrossRef](#)]
34. Myneni, R.B.; Keeling, C.D.; Tucker, C.J.; Asrar, G.; Nemani, R.R. Increased plant growth in the northern high latitudes from 1981 to 1991. *Nature* **1997**, *386*, 698–702. [[CrossRef](#)]
35. Piao, S.; Wang, X.; Ciais, P.; Zhu, B.; Wang, T.; Liu, J. Changes in satellite-derived vegetation growth trend in temperate and boreal Eurasia from 1982 to 2006. *Glob. Chang. Biol.* **2011**, *17*, 3228–3239. [[CrossRef](#)]
36. Pan, J.; Wang, M.; Li, D.; Li, J. Automatic Generation of Seamline Network Using Area Voronoi Diagrams With Overlap. *IEEE Trans. Geosci. Remote Sens.* **2009**, *47*, 1737–1744. [[CrossRef](#)]
37. Hansen, M.C.; Loveland, T.R. A review of large area monitoring of land cover change using Landsat data. *Remote Sens. Environ.* **2012**, *122*, 66–74. [[CrossRef](#)]
38. *USGS Product Guide Provisional Landsat 8 Surface Reflectance Product*; Department of the Interior U.S. Geological Survey: Sunrise Valley Drive Reston, VA, USA, 2015; pp. 1–27.
39. Ju, J.; Roy, D.P.; Vermote, E.; Masek, J.; Kovalsky, V. Continental-scale validation of MODIS-based and LEDAPS Landsat ETM+ atmospheric correction methods. *Remote Sens. Environ.* **2012**, *122*, 175–184. [[CrossRef](#)]
40. Sexton, J.O.; Song, X.-P.; Huang, C.; Channan, S.; Baker, M.E.; Townshend, J.R. Urban growth of the Washington, D.C.–Baltimore, MD metropolitan region from 1984 to 2010 by annual, Landsat-based estimates of impervious cover. *Remote Sens. Environ.* **2013**, *129*, 42–53. [[CrossRef](#)]
41. Roscher, R.; Förstner, W.; Waske, B. I²Vm: Incremental import vector machines. *Image Vis. Comput.* **2012**, *30*, 263–278. [[CrossRef](#)]
42. Braun, A.C.; Weidner, U.; Hinz, S. Classification in high-dimensional feature spaces—assessment using SVM, IVM and RVM with focus on simulated EnMAP data. *IEEE J. Sel. Top. Appl. Earth Obs. Remote Sens.* **2012**, *5*, 436–443. [[CrossRef](#)]
43. Suess, S.; van der Linden, S.; Leitao, P.J.; Okujeni, A.; Waske, B.; Hostert, P. Import Vector Machines for Quantitative Analysis of Hyperspectral Data. *IEEE Geosci. Remote Sens. Lett.* **2014**, *11*, 449–453. [[CrossRef](#)]
44. Braun, A.C.; Weidner, U.; Hinz, S. Support vector machines, import vector machines and relevance vector machines for hyperspectral classification—A comparison. In Proceedings of the IEEE 3rd Workshop on Hyperspectral Image and Signal Processing: Evolution in Remote Sensing (WHISPERS), Lisbon, Portugal, 6 June 2011; pp. 1–4.
45. Roscher, R.; Waske, B.; Forstner, W. Kernel discriminative Random fields for land cover classification. In Proceedings of the 2010 IAPR Workshop on Pattern Recognition in Remote Sensing (PRRS), Istanbul, Turkey, 22 August 2010.
46. Hu, X.; Weng, Q. Estimating impervious surfaces from medium spatial resolution imagery using the self-organizing map and multi-layer perceptron neural networks. *Remote Sens. Environ.* **2009**, *113*, 2089–2102. [[CrossRef](#)]

47. Flood, N. Continuity of Reflectance Data between Landsat-7 ETM+ and Landsat-8 OLI, for Both Top-of-Atmosphere and Surface Reflectance: A Study in the Australian Landscape. *Remote Sens.* **2014**, *6*, 7952–7970. [[CrossRef](#)]
48. Roy, D.P.; Kovalsky, V.; Zhang, H.K.; Vermote, E.F.; Yan, L.; Kumar, S.S.; Egorov, A. Characterization of Landsat-7 to Landsat-8 reflective wavelength and normalized difference vegetation index continuity. *Remote Sens. Environ.* **2016**, *185*, 57–70. [[CrossRef](#)]
49. Dorais, A.; Cardille, J. Strategies for incorporating high-resolution google earth databases to guide and validate classifications: Understanding deforestation in Borneo. *Remote Sens.* **2011**, *3*, 1157–1176. [[CrossRef](#)]
50. Cunningham, S.; Rogan, J.; Martin, D.; DeLauer, V.; McCauley, S.; Shatz, A. Mapping land development through periods of economic bubble and bust in Massachusetts using Landsat time series data. *GIScience Remote Sens.* **2015**, *52*, 397–415. [[CrossRef](#)]
51. Sun, G.; Chen, X.; Jia, X.; Yao, Y.; Wang, Z. Combinational Build-Up Index (CBI) for Effective Impervious Surface Mapping in Urban Areas. *IEEE J. Sel. Top. Appl. Earth Obs. Remote Sens.* **2016**, *9*, 2081–2092. [[CrossRef](#)]
52. Bagan, H.; Yamagata, Y. Land-cover change analysis in 50 global cities by using a combination of Landsat data and analysis of grid cells. *Environ. Res. Lett.* **2014**, *9*, 064015. [[CrossRef](#)]
53. Zhu, Z.; Woodcock, C.E. Continuous change detection and classification of land cover using all available Landsat data. *Remote Sens. Environ.* **2014**, *144*, 152–171. [[CrossRef](#)]
54. Congalton, R.G. Accuracy assessment and validation of remotely sensed and other spatial information. *Int. J. Wildl. Fire* **2001**, *10*, 321–328. [[CrossRef](#)]
55. Gislason, P.O.; Benediktsson, J.A.; Sveinsson, J.R. Random forests for land cover classification. *Pattern Recognit. Lett.* **2006**, *27*, 294–300. [[CrossRef](#)]
56. Sundarakumar, K.; Harika, M.; Begum, S.K.A.; Yamini, S.; Balakrishna, K. Land Use And Land Cover Change Detection And Urban Sprawl Analysis Of Vijayawada City Using Multitemporal Landsat. *Int. J. Eng. Sci. Technol.* **2012**, *4*, 170–178.
57. Luo, J.; Du, P.; Alim, S.; Xie, X.; Xue, Z. Annual Landsat analysis of urban growth of Nanjing City from 1980 to 2013. In Proceedings of the 2014 3rd International Workshop on Earth Observation and Remote Sensing Applications (EORSA), Changsha, China, 11–14 June 2014; pp. 357–361.
58. *Western Australian Planning Commission Draft State Planning Policy 1, State Planning Framework (Variation No. 3)*; Department of Planning, Government of Western Australia: Perth, WA, Australia, 2016.
59. *Western Australian Planning Commission Development Control Policy 1.9*; Department of Planning, Government of Western Australia: Perth, WA, Australia, 2010; pp. 1–5.
60. *Western Australian Planning Commission Western Australian Planning Commission Urban Growth Monitor: Perth Metropolitan, Peel and Greater Bunbury Regions 2016*; Department of Planning, Government of Western Australia: Perth, WA, Australia, 2016.
61. *Western Australian Planning Commission Urban Growth Monitor: Perth Metropolitan, Peel and Greater Bunbury Regions 2012*; Department of Planning, Government of Western Australia: Perth, WA, Australia, 2012.
62. Perry, M.; Rowe, J.E. Fly-in, fly-out, drive-in, drive-out: The Australian mining boom and its impacts on the local economy. *Local Econ.* **2014**, *30*, 139–148. [[CrossRef](#)]
63. *Western Australian Planning Commission Central Sub-Regional Planning Framework*; Department of Planning, Government of Western Australia: Perth, WA, Australia, 2015.
64. *Western Australian Planning Commission North-West Sub-Regional Planning Framework*; Department of Planning, Government of Western Australia: Perth, WA, Australia, 2015.
65. *Western Australian Planning Commission North-East Sub-Regional Planning Framework*; Department of Planning, Government of Western Australia: Perth, WA, Australia, 2015.
66. *Western Australian Planning Commission South Metropolitan Peel Planning Framework*; Department of Planning, Government of Western Australia: Perth, WA, Australia, 2015.
67. *Western Australian Planning Commission Delivering Directions 2031 Report Card 2014*; Department of Planning, Government of Western Australia: Perth, WA, Australia, 2014.
68. Miller, R.B.; Small, C. Cities from space: Potential applications of remote sensing in urban environmental research and policy. *Environ. Sci. Policy* **2003**, *6*, 129–137. [[CrossRef](#)]

69. Pravitasari, A.E.; Saizen, I.; Tsutsumida, N.; Rustiadi, E.; Pribadi, D.O. Local Spatially Dependent Driving Forces of Urban Expansion in an Emerging Asian Megacity: The Case of Greater Jakarta (Jabodetabek). *J. Sustain. Dev.* **2015**, *8*, 108–120. [[CrossRef](#)]
70. Seto, K.; Fragkias, M.; Guneralp, B.; Reilly, M. A next-generation approach to the characterization of a non-model plant transcriptome. *Curr. Sci.* **2011**, *101*, 1435–1439.
71. Marfai, M.A.; Sekaranom, A.B.; Ward, P. Community responses and adaptation strategies toward flood hazard in Jakarta, Indonesia. *Nat. Hazards* **2014**, *75*, 1127–1144. [[CrossRef](#)]
72. Suryahadi, A.; Sumarto, S. Poverty and Vulnerability in Indonesia before and after the Economic Crisis. *Asian Econ. J.* **2003**, *17*, 45–64. [[CrossRef](#)]



© 2017 by the authors; licensee MDPI, Basel, Switzerland. This article is an open access article distributed under the terms and conditions of the Creative Commons Attribution (CC BY) license (<http://creativecommons.org/licenses/by/4.0/>).